

## Coupling 3D modelling and forward-inverse modelling of potential field data (gravity and magnetic data).

Aurore Joly, Antonio Guillen, Philippe Calcagno, Gabriel Courrioux

► **To cite this version:**

Aurore Joly, Antonio Guillen, Philippe Calcagno, Gabriel Courrioux. Coupling 3D modelling and forward-inverse modelling of potential field data (gravity and magnetic data).. GIS in geology, Nov 2006, Moscou, Russia. 6p. hal-00107327

**HAL Id: hal-00107327**

**<https://hal-insu.archives-ouvertes.fr/hal-00107327>**

Submitted on 18 Oct 2006

**HAL** is a multi-disciplinary open access archive for the deposit and dissemination of scientific research documents, whether they are published or not. The documents may come from teaching and research institutions in France or abroad, or from public or private research centers.

L'archive ouverte pluridisciplinaire **HAL**, est destinée au dépôt et à la diffusion de documents scientifiques de niveau recherche, publiés ou non, émanant des établissements d'enseignement et de recherche français ou étrangers, des laboratoires publics ou privés.

# COUPLING 3D MODELLING AND FORWARD-INVERSE MODELLING OF POTENTIAL FIELD DATA (GRAVITY AND MAGNETIC DATA)

**Joly Aurore**<sup>(1,2)</sup> ([a.joly@brgm.fr](mailto:a.joly@brgm.fr)), **Guillen Antonio**<sup>(1)</sup> ([a.guillen@brgm.fr](mailto:a.guillen@brgm.fr)), **Calcagno Philippe**<sup>(1)</sup> ([p.calcagno@brgm.fr](mailto:p.calcagno@brgm.fr)), **Courrioux Gabriel**<sup>(1)</sup> ([g.courrioux@brgm.fr](mailto:g.courrioux@brgm.fr))

*1)Bureau de Recherches Géologiques et Minières, 3 av. C. Guillemin, BP 6009, 45060 Orléans Cedex 2, France*

*2)ISTO, UMR CNRS 6113, Université Orléans F 45067 Cedex 2, France*

## 1. Introduction

The 3D modeling of geological objects is often decomposed in two steps: i) delimitation of the boundaries of the units corresponding to the various geological formations or ore types; and ii) verification and estimation of these boundaries using geophysical data. A new approach using potential-field interpolators addressing the 3D modeling problem is used here (Ch.Lajaunie et al. 1997). We will discuss how we can statistically estimate the validity of such 3D model taking in account various geophysical data. This estimation can be computed by inverting complementary datasets, provided (a) the data are a function of the 3D distribution of a source, (b) the response of a given 3D source distribution can be calculated, and (c) the source distribution shows some degree of correlation with the litho-regions. Gravity and magnetic potential field data generally satisfy these criteria. Unfortunately, these data do not allow source geometry to be uniquely resolved through inversion, nor is the source geometry likely to be perfectly correlated with the litho-regions. Even allowing for these limitations, we can see through the expression for the posterior probability density function (PPD) for a Bayesian inversion procedure how uncertainty in prior geological knowledge is modified by investigating the fit to observed potential field data for various models;

$$P(\mathbf{m} | \mathbf{d}_o) = k\rho(\mathbf{m})L(\mathbf{d}_o | \mathbf{m}) \quad (1)$$

where  $k$  is a normalizing constant,  $\rho(\mathbf{m})$  is the prior probability for the property model  $\mathbf{m}$  based on geological knowledge, and  $L(\mathbf{d}_o | \mathbf{m})$  is the likelihood function that reflects the agreement between the observed potential field response and the predicted response of the model. Litho-models that have reasonable probability based on prior knowledge are downgraded if the likelihood deduced from the associated potential field response is very low.

To reduce the non-uniqueness, we can add to the classical data, the tensor components of the field. The main goal with gradients measurements is to improve accuracy and spatial resolution of gravity and magnetic surveys. For those reasons, we propose to build a 3D forward modelling and inversion method for tensor data.

## 2. Constrained Potential Field Inversion Overview

The geological model is discretized into a 3D matrix of cells, termed voxels, to produce an initial rock unit ('lithology') model. Lithology is the primary model parameter. The lithology associated with subsurface voxels information is free to vary, subject to the condition that the "shape trend" of the initial model remains unchanged. The inversion explores variations to the initial model which reproduce the supplied gravity or magnetic data to within a desired tolerance level. The adopted strategy is to randomly walk around the space of possible models for a given set of a priori information. This approach was proposed by Mosegaard and Tarantola (1995) and developed in 2D by Bosch et al. (2001). At each iteration, we make one of two possible changes. The physical property (density and/or magnetic susceptibility and/or remnant magnetization) for a randomly selected voxel that is separated from the boundary of that unit may be modified. Alternately, the lithology of a voxel that lies on the interface between two or more units may be modified and a new physical property assigned to that voxel according to a random selection from the probability function of the relevant physical property distribution for the new lithology. The voxels to which the latter operation can be applied is restricted by the constraint that the "shape trend" of the model is not altered. The change in the misfit between the observed gravity and/or magnetic field and/or tensor components data and the responses calculated for the modified model is determined. This change is examined in a probabilistic framework to determine whether the modification to the model is accepted.

### 2.1. Detailed Outline of the Inversion Algorithm

The inversion algorithm can be defined using 11 steps.

1. Build the a priori geological model
2. Define the a priori physical property laws
3. Discretise this model
4. Compute topology
5. Make a list of the boundary or frontier cells
6. Compute the gravity and/or magnetic field and gravity and/or magnetic tensor for each cell
7. Initialise the density or magnetisation values
8. Compute the geophysical effects of the model
9. Disturb the model
10. Compute the geophysical effects of the disturbed model
11. Compute the likelihoods of the disturbed model
- 12.

During the initial part of the inversion, the data misfit for each field of the current model follows a generally decreasing trend. At some point, the data misfit reaches an asymptotic value, defined or set in function of the measurement errors and we begin to store the models. These stored models are an exploration of the probability space of acceptable models. After completing Step 11, the inversion returns to Step 9 and continues to iterate around this loop. An ensemble of models that can satisfactorily explain the geophysical signature might be explored by continuing for a further million iterations.

During the inversion process, at the step 9, we will use after some iteration an operation to homogenise the current model. We will use the morphology-based operations erosion, dilation and their combined uses to add or remove voxels from the boundaries of features in order to smooth them, to join separated portions of features or separate touching features, and to remove isolated voxels noise from the model. Dilation turns

voxels "on" according to rules based on the number or arrangement of neighbouring voxels, erosion turns pixels "off" according to similar rules, while Opening - an erosion followed by a dilation - and Closing - the reverse sequence - attempt to restore the original area of features but with some rearrangement of the boundary pixels. We apply these operations during some state of the step 9 during the inversion process, they control the "quality" of the model.

To modify the geometry of the bodies we apply a growing and thinning geological units methods, after a given number of iterations. For this purpose, we will use the previous method to modify the shape of the geological units using growing (dilation process) or thinning (erosion process). These operations occur during step 9. After a random number of inversion we select randomly a geological unit, a process (growing or thinning) and one of the six possible directions (N, S, E, W, Up, Down) to realise this shape modification.

Once inversion finished, the set of stored model allows to compute for each voxel, the probability of finding each unit, the most probable lithology and the mean value of the petrophysical properties.

### **3. Application to the Montmarault granitic massif in the Variscan French Massif Central.**

Montmarault porphyritic granite in the northern part of the French Massif Central is located along the Sillon Houiller Fault (SHF). Field structural observation, U-Th/Pb dating, petrographic and magnetic fabric results described in Part I of this study demonstrated that the Montmarault pluton, emplaced at the Namurian (about 320 Ma), is controlled by the NW-SE maximum stretching direction, also well recorded by emplacement fabric of other Namurian granitic pluton of the French Massif Central. However, foliation and lineation patterns provide insufficient information to determine an accurate three dimensional shape of a granitic pluton, thus, the use of joint gravity and magnetic methods becomes essential, despite interpretations are not always unique.

To constrain the structure of the granitic massif, new gravity measurements have been acquired from 525 stations. Supplemented to existing gravity data, we provide an average coverage of the area with about 1 station per km<sup>2</sup>. As suggesting Bouguer anomaly and magnetic intensity maps, the important negative gravity and magnetic anomalies are well located along the SHF and correlated to the thickening of the granite in relation with tectonic structure. To the west of the SHF, the important positive V-shaped magnetic and gravity anomalies suggest the thinner laccolith granite with high magnetic susceptibility and low density is probably underlain by geologically evidenced intrusions of diorite with high magnetic susceptibility and density. The late Paleozoic sedimentary grabens are characterised by both negative gravity and magnetic anomalies.

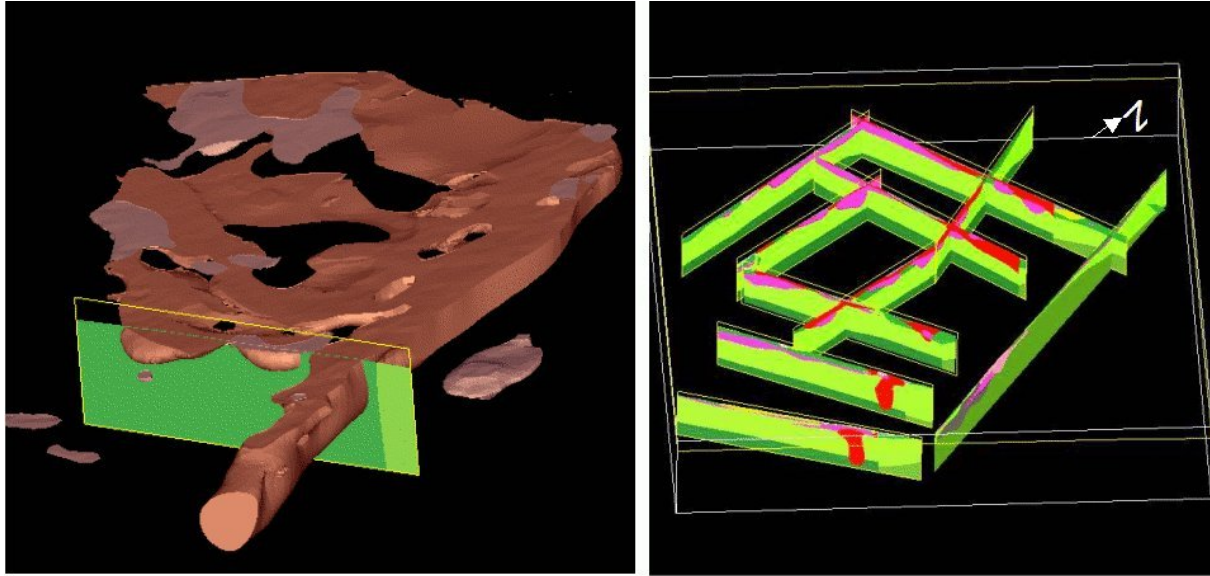


Fig. 1 - On the left the 3D model in red the granites and in pink the leucogranites. The SHF is the East limit of the granites. On the right we have the 3D view of different sections used to build the model.

Geophysical and new structural information have been integrated to construct 3D model to better understand the emplacement of Montmarault granite, this model contains 30 different geological units and faults (Fig. 1). From this starting model, we have applied the previous inverse method, we obtain a set (1000 000 of different models) explaining the both gravity and magnetic anomalies, taking in account the petrophysical data (densities, susceptibilities and remanant magnetization), and close to the 3D starting model. The figure 2 shows the agreement between the fields created by the model and the measurements, just after 330000 iterations.

The results (Fig 3) show that the granites thickness increases with a high probability along the SHF, the joint inversion of gravity and magnetic inversion add constrains on the granites where the magnetic diorites bound them.

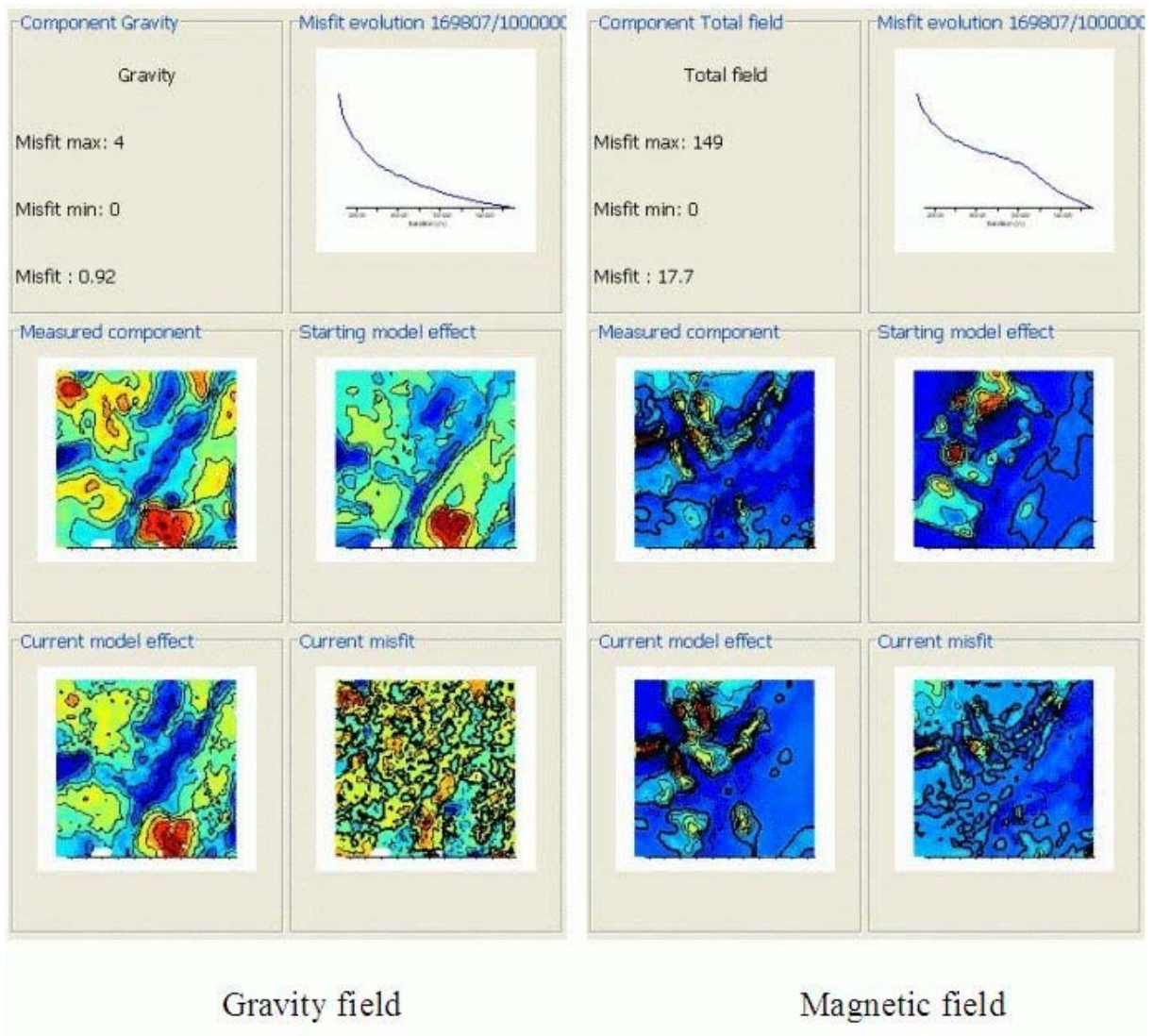


Fig. 2 - Misfit evolution after 330000 iterations of the gravity and magnetic fields.

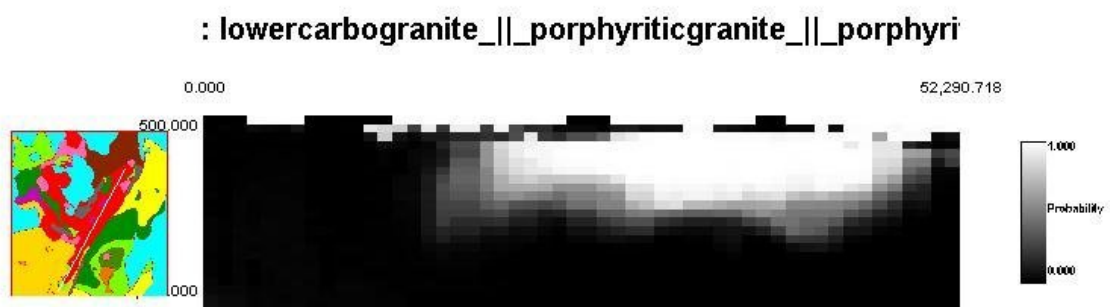


Fig. 3 - Probability ( $P=1$  in white,  $P=0$  in black) to have the granite units along a cross-section SW-NE along the SHF. We see that the thickness of the granite units increase from south to north.

## REFERENCES

1. Bosch M., Guillen A. and Ledru P., 2001, Lithologic tomography: an application to geophysical data from the cadomian belt of northern Brittany, France: *Tectonophysics*, 331, 197-228.
2. Mosegaard K., and Tarantola A., 1995, Monte Carlo sampling of solutions to inverse problems: *J. Geophys. Res.*, 100, No. B7, 124321-12447.
3. Lajaunie Ch., Courrioux G., Manuel L. 1997, Foliation fields and 3d cartography in geology: principles of a method based on potential interpolation. *Mathematical Geology*, 29, 571-584.